J Membrane Biol (2010) 235:27–41
DOI 10.1007/s00232-010-9253-6

Functional Characterization of a ClC-2-Like Cl^- Conductance in Surface Epithelial Cells of Rat Rectal Colon

Akihiro Inagaki · Soichiro Yamaguchi · Hiromi Takahashi-Iwanaga · Toshihiko Iwanaga · Toru Ishikawa

Received: 27 December 2009 / Accepted: 28 March 2010 / Published online: 22 April 2010

Abstract ClC-2, a member of the voltage-gated Cl^- channel family, is expressed in the distal colonic surface epithelial cells of various species, but its functional significance remains unclear. Here, by means of electrophysiological and molecular biological techniques, we have identified and characterized a ClC-2-like conductance naturally expressed by surface epithelial cells acutely dissociated from rectal colon of rats fed a standard diet. Whole-cell patch-clamp experiments showed that the surface cells, whether an amiloride-sensitive Na^+ conductance was present or not, displayed a strong hyperpolarization-activated, inwardly rectifying Cl^- current. Analysis both by in situ hybridization and immunohistochemistry confirmed the expression of ClC-2 in the rectal surface epithelium. The native Cl^- current shared common electrophysiological properties including voltage-dependent activation, anion selectivity sequence, and Zn^{2+} sensitivity with that recorded from HEK293 cells transfected with ClC-2 cloned from rat rectal colon (rClC-2). Cell-attached patch recordings on the surface cells revealed that native ClC-2-like currents activated only at potentials at least 40 mV more negative than resting membrane potentials. In Ussing chamber experiments with rat rectal mucosa, either basolateral or apical application of Zn^{2+} (0.1 mM), which inhibited both native ClC-2-like currents and recombinant rClC-2 currents, had little, if any, effects on basal amiloride-sensitive short-circuit current. Collectively, these results not only demonstrate that a functional ClC-2-type Cl^- channel is expressed in rat rectal surface epithelium, but also suggest that the channel activity may be negligible and thus nonessential for controlling electrogenic Na^+ transport in this surface epithelium under basal physiological conditions.

Keywords Inwardly rectifying Cl^- current · Distal colon · Patch clamp · Electrogenic Na^+ absorption

A. Inagaki · S. Yamaguchi · T. Ishikawa
Laboratory of Physiology, Department of Biomedical Sciences, Graduate School of Veterinary Medicine, Hokkaido University, Sapporo 060-0818, Japan

A. Inagaki
Department of Physiology, Institute of Health Biosciences, The University of Tokushima Graduate School, Tokushima 770-8503, Japan

H. Takahashi-Iwanaga · T. Iwanaga
Laboratory of Histology and Cytology, Graduate School of Medicine, Hokkaido University, Sapporo 060-8638, Japan

Present Address:
T. Ishikawa (✉)
Division of Biomedical Science, Department of Basic Veterinary Medicine, Obihiro University of Agriculture and Veterinary Medicine, Obihiro 080-8555, Japan
e-mail: torui@obihiro.ac.jp

Surface epithelium of mucosa contributes to salt and water absorption of mammalian distal colon. Although the underlying cellular mechanism of this absorptive process is largely dependent on species, segments, and experimental conditions used, it is believed that transepithelial ion transport, which is followed by osmotic water flow, requires the coordinated activities of Cl^- channels as well as other ion-transporting proteins (Kunzelmann and Mall 2002; Geibel 2005). Besides a KCl cotransporter and Cl^-/HCO_3^- exchanger, Cl^- channels are proposed to constitute a basolateral Cl^- efflux pathway in the electroneutral NaCl absorption process, where Na^+ and Cl^- ions enter the cytosol across the apical membrane of surface epithelium via a Na^+/H^+ exchanger and Cl^-/HCO_3^- exchanger, respectively (Kunzelmann and Mall 2002; Geibel 2005).

Basolateral Cl^- channels, in addition to the paracellular Cl^- shunt, are also suspected to be responsible for an exit pathway of Cl^- ions that might enter the cell via apical Cl^- channels (e.g., cystic fibrosis transmembrane conductance regulator; CFTR) in the electrogenic Na^+ absorption process, where the epithelial Na^+ channels (ENaC) mediate the rate-limiting apical Na^+ influx (Kunzelmann and Mall 2002; Geibel 2005). However, little is known about molecular nature of basolateral Cl^- channels and their relative contribution to the transport processes in surface epithelium of distal colon.

ClC-2, a member of the voltage-gated Cl^- channel (ClC) family, forms a hyperpolarization-activated, inwardly rectifying Cl^- conductance in the plasma membrane (Thiemann et al. 1992; Jentsch et al. 2002). Previous immunocytochemical studies indicated that ClC-2 is predominantly located in the basolateral membrane of surface cells of distal colon in rats, guinea pigs, and mice (Catalán et al. 2002; Lipecka et al. 2002; Peña-Münzenmayer et al. 2005), although different localization has been also reported for human distal colon (Lipecka et al. 2002) and for murine and porcine small intestine (Gyömörey et al. 2000; Moeser et al. 2004). In addition to these accumulating molecular data, previous whole-cell patch-clamp and Ussing chamber studies on guinea pig distal colon showed that a Cd^{2+}-sensitive, hyperpolarization-activated, inwardly rectifying Cl^- conductance or a Cd^{2+}-sensitive Cl^- conductance is present in surface cells (Catalán et al. 2002) or the basolateral aspect of the epithelium (Catalán et al. 2004), respectively. Therefore, ClC-2 has been a good candidate for the Cl^- channel that might be involved in transepithelial NaCl absorption in the surface cells.

Interestingly, however, any deficits in absorptive function of distal colon have not been noted in ClC-2 knockout (KO) mice, in which severe degeneration of the testes and retina was evident (Bösl et al. 2001; Nehrke et al. 2002). Zdebik et al. (2004) have observed no alterations in either morphology or basal transepithelial ion transport (as assessed by short-circuit current [I_{sc}]) of the colonic epithelium in the ClC-2 KO mice fed a normal-salt diet. These investigators also found no significant changes in basal amiloride-sensitive I_{sc} ($I_{sc\text{-}amil}$) in the KO mice fed a low-salt diet, a maneuver that upregulates the electrogenic Na^+ absorption (Zdebik et al. 2004). Although the possibility that genetic disruption of ClC-2 might cause compensatory changes in other basolateral Cl^- efflux pathways cannot be completely excluded, these results raise the question of whether the ClC-2 would be active enough to play a major role in absorptive function under normal physiological conditions, and/or of whether the relative contribution of ClC-2 to the colonic epithelial transport might vary in different species, segments, and experimental conditions. Nevertheless, as mentioned above, functional properties of a native ClC-2-like conductance in distal colonic surface cells have not been studied in most species except guinea pigs (Catalán et al. 2002, 2004).

We have previously shown that rectal colonic epithelium of rats fed a standard-salt diet displays an amiloride-sensitive electrogenic Na^+ transport under basal conditions, and that the rectal surface epithelial cells exhibit an amiloride-sensitive whole-cell Na^+ conductance, which is most likely mediated by ENaC (Inagaki et al. 2004a). The basal $I_{sc\text{-}amil}$ in the rectal colon was approximately 30–40 $\mu A/cm^2$ (which corresponds to approximately 1 $\mu Eq\ h^{-1}\ cm^{-2}$) (Inagaki et al. 2004a), amplitudes being also comparable to that observed in the guinea pig (Clauss et al. 1985; Catalán et al. 2004) and mice (Bachhuber et al. 2008) distal colon under normal conditions, while the electroneutral Na^+ transport process would be dominant (Binder and Sandle 1994). ClC-2 was particular interest to us because the channel, if significantly active, might contribute to the electrical properties of the rectal surface cells and thus to the overall electrogenic Na^+ transport under resting conditions—for example, by modulating the membrane potential (thus electrochemical driving force of Na^+ influx through ENaC) and/or by influencing the intracellular Cl^- concentration that might control overall ENaC activity, as shown in other native and heterologous expression systems (Dinudom et al. 1993; Kunzelmann 2003; Xie and Schafer 2004; Gu 2008). In view of this, it is noteworthy that a ClC-2-like Cl^- conductance has been found in other native epithelia, where the ENaC-mediated electrogenic Na^+ absorption occurs (Dinudom et al. 1993; Fischer et al. 2007). Nonetheless, the physiological effects on electrogenic Na^+ transport remain uncertain. In fact, recent data in ClC-2 KO mice provided little support for an essential role of ClC-2 in NaCl absorption of mouse salivary ductal epithelium (Romanenko et al. 2008).

The aim of the present study was to identify and characterize a ClC-2-like Cl^- conductance naturally expressed in rat rectal surface epithelial cells, and to examine whether the channel could be active and contribute largely to electrogenic Na^+ absorptive function of these cells under basal conditions. Some preliminary results have been presented in part to the 81st annual meeting of the Physiological Society of Japan (Inagaki et al. 2004b).

Materials and Methods

All experiments were performed in accordance with a protocol approved by the Committee on Animal Experimentation, Graduate School of Veterinary Medicine, Hokkaido University.

Patch-Clamp Analyses

Male Sprague-Dawley rats (5 weeks old) purchased from Clea Japan (Tokyo, Japan) were fed a standard rat diet (Labo MR Standard; Nosan, Yokohama, Japan) and water ad libitum at least more than 2 weeks until used. Animals (180–450 g; 324 ± 5 g, $n = 123$) were immediately humanely killed by cervical dislocation, and distal colon (with rectal colon) was rapidly removed and rinsed with a standard NaCl solution (pH 7.4 adjusted with NaOH) containing (mM): NaCl (145), KCl (5), $CaCl_2$ (1), $MgCl_2$ (1), HEPES (N-[2-hydroxyethyl] piperazine-N′[2-ethanesulfonic acid]) (10), and D-glucose (10). The rectal colon (RC) used in the present study corresponds to RC1 and RC2 segments, which have been shown to exhibit an amiloride-sensitive electrogenic Na^+ transport under basal conditions (Inagaki et al. 2004a).

The preparation of rectal colonic crypts has been described elsewhere (Inagaki et al. 2004a). Current recordings were made by means of the standard patch-clamp techniques from surface epithelial cells surrounding orifices of the isolated crypts as described elsewhere (Inagaki et al. 2004a) and from HEK293 cells stably expressing ClC-2 cloned from rat rectal mucosa (rClC-2). In experiments where the effects of Zn^{2+} on native inwardly rectifying Cl^- currents were examined, the data obtained from the cells, which were likely dissociated from surface epithelium of crypts, were also pooled and presented. An Axopatch-1D patch-clamp amplifier (Axon Instruments, Union City, CA) was used to measure whole-cell and cell-attached patch currents. The amplifier was driven by pCLAMP 6.0 software (Axon Instruments) to allow the delivery of voltage-step protocols with concomitant digitization of the currents. Current–voltage (I–V) relations were usually studied with 10 (or 20) mV voltage pulses, each 800 ms in duration, delivered at command voltages between −200 and +40 mV, and voltage pulses were separated by 10–30 s, during which the cell potential was held at 0 mV, unless otherwise stated. The currents were filtered through an internal four-pole Bessel filter at 500 Hz, sampled at 1 or 2 kHz, and stored directly into the computer's hard disk through a Digidata 1200 interface (Axon Instruments). Subsequent data analysis was performed by Clampfit supplied with pCLAMP 6.0 (Axon Instruments) and Origin 4.10 (Microcal software, Northampton, MA). The patch-clamp pipettes had resistances of 5–8 MΩ and 2–3 MΩ for the surface cells and HEK293 cells, respectively, when filled with a standard Cs-glutamate-rich solution described below. The cell capacitance (W_C) of rectal surface cells used was 11.1 ± 0.4 pF ($n = 132$). The values are similar to those reported for surface cells of rat colonic crypts, where there is no evidence for cell-to-cell coupling (Jacobi et al. 1998). The series resistance (R_S) in these studies, which was 22.2 ± 0.5 MΩ ($n = 132$), was not compensated. In experiments that used HEK293 cells, W_C and R_S were 17.9 ± 0.7 pF ($n = 90$) and 6.9 ± 0.3 MΩ ($n = 90$), respectively. The pipette potential was corrected for the liquid junction potentials as described elsewhere (Inagaki et al. 2004a). All experiments were performed at room temperature.

Time courses for current activation were fit to single or double exponential plus a constant term equation of the form as follows:

$$I(t) = A_1 \exp(-t/\tau_1) + A_2 \exp(-t/\tau_2) + C, \quad (1)$$

where A_1, A_2, and C are current amplitudes and τ_1 (τ_{fast}) and τ_2 (τ_{slow}) are time constants. Voltage dependency of current activation was assessed in experiments as shown in Fig. 2A. After stepping the voltage to various test values, current activation was monitored at a constant "tail" voltage. The tail current that was usually measured several milliseconds (to minimize errors due to transient capacitance current, which was incompletely compensated) after the beginning of a pulse to this voltage was fitted to a Boltzmann distribution of the form as follows:

$$I = I_0 + (I_{max} - I_0)/\{1 + \exp[(V - V_{0.5})/k]\}, \quad (2)$$

where I, I_0, and I_{max} are current as a function of voltage, residual current independent of voltage, and the current (extrapolated) at maximal activation, respectively. $V_{0.5}$ is the voltage of half-maximal activation, and k is the slope factor. On the basis of the assumption that the current was only carried by these monovalent anions, the permeability ratio (P_X/P_{Cl}) was also calculated from the shift in reversal potential (ΔE_{rev}) when external Cl^- is mostly replaced by monovalent anion X^-; that is,

$$\Delta E_{rev} = RT/F \times \ln {P_{Cl}}^1[Cl^-]_o/({P_{Cl}}^2[Cl^-]_o + P_X[X^-]_o), \quad (3)$$

where ${}^1[Cl^-]_o$ is the original extracellular Cl^- concentration and ${}^2[Cl^-]_o$ and $[X^-]_o$ are the extracellular concentrations of Cl^- and the foreign anion X^-, respectively, after the replacement of external solution.

The pipette solution contained (in mM): Cs-glutamate, N-methyl-D-glucamine (NMDG)-glutamate or NMDG-Cl (120), CsCl or NMDG-Cl (10), $MgCl_2$ (1), HEPES (10), and EGTA (Ethylene glycol-bis(2-aminoethylether)-N,N,N′,N′-tetraacetic acid) (10). In some cell-attached and inside-out patch experiments in HEK293 cells, we also used the pipette solution containing (in mM): NMDG-Cl (145), $MgCl_2$ (1), and HEPES (10). The pH of the solution was adjusted with CsOH or NMDG at 7.4. In some experiments, we also used pipette solutions having various Cl^- concentrations, which were prepared by using the Cs-glutamate-rich solution described above and a CsCl-rich solution (pH 7.4

adjusted with CsOH) (mM): CsCl (130), $MgCl_2$ (1), HEPES (10), and EGTA (10). The cells were initially immersed in a bath solution (pH 7.4) containing (in mM): NaCl (145), KCl (5), $MgCl_2$ (1), $CaCl_2$ (1), D-glucose (10), and HEPES (10). In some experiments, the bath solution was changed to the one (pH 7.4) containing (in mM): NaCl, NaBr, NaI, Na-glutamate, NMDG-Cl, NMDG-Br, or NMDG-glutamate (145), $MgCl_2$ (1), and HEPES (10). The pH of the solution was adjusted with NaOH or NMDG.

Transepithelial Current Measurements

Stripped mucosa prepared as described elsewhere (Inagaki et al. 2004a) was mounted in a modified Ussing chamber with a tissue holder (EasyMount Chamber; Physiologic Instruments, San Diego, CA) having an aperture surface area of 0.5 cm^2 and bathed bilaterally in a solution (pH 7.4) that consisted of (in mM): NaCl (115), KCl (5), $CaCl_2$ (1), $MgCl_2$ (1), $NaHCO_3$ (25), HEPES (10, pH 7.4, adjusted with NaOH), and D-glucose (10). Indomethacin (10 μM) was added to the solutions bathing serosal surfaces to minimize prostaglandin production that stimulates cAMP-dependent Cl^- secretion. The bathing solution was continuously gassed with a mixture of 95% O_2–5% CO_2 and had a pH of 7.4. The luminal and basolateral sides of the epithelium were perfused with the bathing solution (at 37°C) continuously at a rate of 1 ml/min (chamber volume of 5 ml). When drugs were applied to either side of the bathing solution, stock solutions were added to provide the desired final concentration, immediately followed by continuous perfusion (1 ml/min) with the solution containing the appropriate concentration of drugs. When drugs were removed, 2.5 ml of the solution was withdrawn from the apical bath and each replaced successively with an equal volume of the standard solution containing no drugs. This procedure was repeated 20 times in parallel to continuous perfusion with drug-free solutions. All preparations were allowed to equilibrate for 40–90 min after mounting on the chambers before the measurements were taken as described previously (Inagaki et al. 2004a).

The tissues were continuously short-circuited to monitor short-circuit current (I_{sc}, μA/cm^2) with a voltage-clamping amplifier (CEZ-9100, Nihon Kohden, Tokyo, Japan) as described elsewhere (Inagaki et al. 2004a). I_{sc} is referred to as positive for current flowing across the epithelium from mucosal side to serosal side. Typically, the transepithelial resistance (R_t) was estimated from the current change in response to bipolar square voltage pulses (±2 mV, 1-s duration) imposed across the mucosa at 5-min intervals. The resistance of the bathing fluid between the voltage-sensing electrodes was measured and compensated by the amplifier before each experiment. To evaluate the effects of Zn^{2+} on basal amiloride-sensitive I_{sc} ($I_{sc\text{-}amil}$) precisely, we proceeded with experiments only when the initial $I_{sc\text{-}amil}$ and R_t values were larger than 15 μA/cm^2 and 50 Ω cm^2, respectively.

Cloning of ClC-2 from Rat Rectal Colon

mRNA was extracted from rat rectal colonic mucosa prepared as described above with TRIzol reagent (Life Technologies, Grand Island, NY) and BioMag mRNA purification kit (Polysciences, Warrington, PA) following the manufacturer's instructions. First-strand cDNA was generated from mRNA with SuperScriptII RT (Life Technologies). The specific oligonucleotide primers for polymerase chain reaction (PCR) for rClC-2 were 5′-AAG CAA GAG GAG GCA AGA GGA C-3′ (nt 136–157; sense) and 5′-TTC TCA AAA GAC GAG GCA GGG G-3′ (nt 3070–3049; antisense), which were derived from the published sequences of the rat ClC-2 (GenBank accession no. NM_017137). The size of the expected fragment was 2935 bp. The PCR reaction was performed with TaKaRa LA Taq (Takara Bio, Otsu, Japan). The PCR conditions were denaturation 94°C for 30 s; annealing 66°C for 30 s; extension 72°C for 4 min; 35 cycles. As a control, β-actin cDNA was amplified with 5′-GACTACCTCATGAAGA TCCT-3′ (sense) and 5′-CCACATCTGCTGGAAGGTGG-3′ (antisense), and 510-bp product was obtained.

On the basis of the complete sequence information of the rat ClC-2 (NM_017137), we amplified from mRNA two overlapping PCR fragments by reverse transcriptase PCR (RT-PCR) with a high-fidelity DNA polymerase (PfuTurbo, Stratagene, La Jolla, CA) with the following primers: 1) 5′-AAG CAA GAG GAG GCA AGA GGA C-3′ (nt 136–157; sense); 5′-ACA GCG AAG AAG GTG GAG GTG A-3′ (nt 1001–980; antisense); 2) 5′-GGG GAG TGG TGC TGA AAG AGT A-3′ (nt 701–722; sense); 5′-TTC TCA AAA GAC GAG GCA GGG G-3′ (nt 3070–3049; antisense). PCR products of the fragments were gel excised, purified, cloned into the pGEM-T Easy vector (Promega, Madison, WI), and sequenced on both strands, and they were found to correspond to the sequence of rat ClC-2. The first fragment linearized by *Eco*RI (in vector)/*Nhe*I (nt 904; start codon at nt 169) and the second fragment by *Nhe*I/*Not*I (in vector) were assembled by double ligation into pCI-neo (Promega) plasmid linearized by *Eco*RI and *Not*I.

Transfection of HEK293 Cells with rClC-2

HEK293 cells stably expressing rClC-2 were generated by transfecting cells with a plasmid construct encoding the rClC-2 and a neomycin resistance gene contained within the mammalian expression vector pCI-neo by using lipofectamine (Life Technologies). G418 (0.8 mg/ml)-resistant colonies were purified and tested for rClC-2 expression by

whole-cell patch clamp. HEK293 cells were also stably transfected with vector alone. HEK293 cells stably transfected with vector alone only exhibited much less whole-cell current (-77.2 ± 12.5 pA [-6.1 ± 1.9 pA/pF] at -97 or -103 mV, $n = 10$) compared with those with the rClC-2 (-5772.4 ± 1005.8 pA [-303.2 ± 57.3 pA/pF] at -97 mV, $n = 11$), when dialyzed with a pipette solution containing 132 mM Cl^- (Cs^+ or $NMDG^+$ as a major cation) in a NaCl-rich bath solution. The cells were then maintained in Dulbecco's modified Eagle's medium supplemented with 10% fetal bovine serum, penicillin (100 units/ml)/streptomycin (0.1 mg/ml), and 0.2 mg/ml G418. The cells were grown at 37°C in a water-saturated 5% CO_2–95% air atmosphere, and passaged 1–2 times weekly. For patch-clamp experiments, the cells were seeded on a cover glass and patched 1–5 days after seeding.

Amiloride, indomethacin, HEPES, and EGTA were obtained from Sigma (St. Louis, MO), and poly-L-lysine was obtained from Nacalai Tesque (Kyoto, Japan). Other chemicals were from Sigma (St. Louis, MO), Sigma-Aldrich Japan (Tokyo, Japan), Wako Chemical (Osaka, Japan), or Nacalai Tesque (Kyoto, Japan). Stock solutions of indomethacin (10 mM) were prepared in ethanol, amiloride (10 mM) in distilled water, and $ZnCl_2$ (1 M or 0.1 M) in 50 mM or 5 mM HCl, respectively.

The results were reported as means ± standard error (SE) of several experiments (n). Statistical significance was evaluated by the two-tailed unpaired and paired Student's t-test. Differences between means were considered to be statistically significance at a value of $P < 0.05$.

In Situ Hybridization and Immunohistochemical Analysis

For in situ hybridization analyses, rats were humanely killed by exposure to CO_2, and fresh tissues were collected from the duodenum, jejunum, ileum, cecum, proximal colon, distal colon, and rectum. They were embedded in a freezing medium (OCT compound; Sakura FineTechnical, Tokyo, Japan) and quickly frozen in liquid nitrogen. Frozen sections, 14 μm in thickness, were prepared in a cryostat and mounted on silicon-coated glass slides. The sections were fixed with 4% paraformaldehyde in 0.1 M phosphate buffer for 15 min and then acetylated with 0.25% acetic anhydride in 0.1 M triethanolamine–HCl (pH 8.0) for 10 min. Hybridization was performed at 42°C for 10 h with a hybridization buffer containing ^{33}P-labeled oligonucleotide probes (10,000 cpm/μl). Two nonoverlapping antisense oligonucleotide DNA probes (45 mer in length) were designed to be complementary to the following sequences: 1121–1165 and 2341–2385 of rat ClC-2 (NM_017137). After hybridization, the sections were rinsed at room temperature for 30 min in 2× standard saline citrate (SSC; 1× SSC: 150 mM sodium chloride, 15 mM sodium citrate) containing 0.1% *N*-lauroylsarcosine sodium, then rinsed twice at 55°C for 40 min in 0.1× SSC containing 0.1% *N*-lauroylsarcosine sodium, dehydrated through a graded series of ethanol, and air dried. Sections were either exposed to BioMax MR film (Kodak, Rochester, NY) for 10 days or dipped in an autoradiographic emulsion (NTB-2; Kodak) at 4°C for 8–10 weeks. The hybridized sections used for autoradiography were counterstained with hematoxylin after development.

In situ hybridization technique using the two nonoverlapping antisense probes for each mRNA exhibited identical labeling in all the tissues examined. The specificity of the hybridization was also confirmed by the disappearance of signals upon the addition of an excess of an unlabeled antisense probe.

For immunohistochemical examination, rats were anesthetized by intraperitoneal injection with sodium pentobarbital (40 mg/kg body weight), and fixed by transcardial perfusion with 4.0% paraformaldehyde buffered at pH 7.3 with 0.1 M phosphate. The proximal colon and the rectum were removed and immersed in the same fixative for 4 h at 4°C. The fixed tissue pieces were equilibrated in a 30% sucrose solution for approximately 6 h at 4°C, quickly frozen in liquid nitrogen, and then sectioned at 8 μm by cryostat. The frozen sections were mounted on glass slides coated with poly-L-lysine, then pretreated with 0.3% Triton X-100 in phosphate-buffered saline (pH 7.2) for 1 h at room temperature to enhance antibody penetration.

Immunohistochemical labeling was performed by the avidin–biotin complex method at room temperature. After blockade of nonspecific binding sites by treatment with 10% normal goat serum for 30 min, the specimens were incubated with a rabbit anti-rat ClC-2 antibody (ACL002; Alomone Laboratories, Jerusalem, Israel) at a dilution of 1:600 overnight, and subsequently with biotinylated goat anti-rabbit IgG (Nichirei, Tokyo, Japan) for 1 h. Visualization of the secondary antibody was achieved with the Vectastain ABC kit (Vector Laboratories, Burlingame, CA) and 0.01% 3,3′-diaminobenzidine with 0.001% H_2O_2. The specificity of immunoreaction on sections was confirmed according to a conventional procedure, including omission of the primary antiserum.

Results

A Slowly Activating, Inwardly Rectifying Cl^- Current in Rat Rectal Surface Cells

Figure 1A(a) shows traces of whole-cell currents, which were elicited by voltage steps between -112 and -22 mV from a holding potential of -12 mV and recorded from a

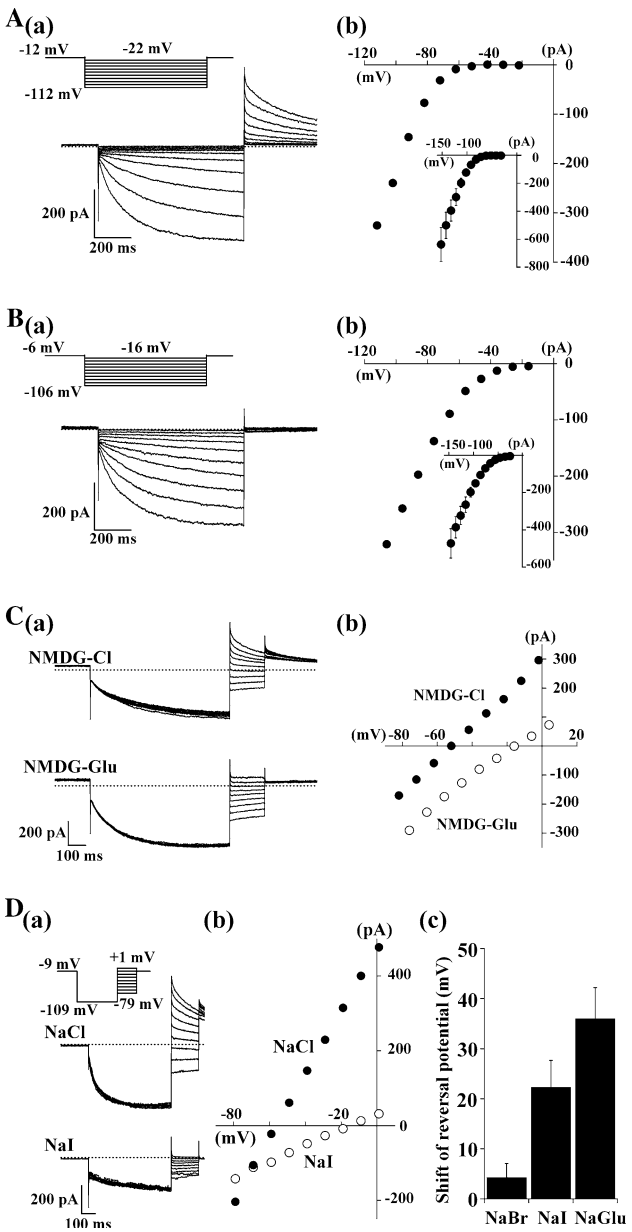

Fig. 1 A slowly activating, inwardly rectifying Cl^- current ($I_{Cl\text{-}IR}$) in surface epithelial cells of rat rectal colon. Whole-cell currents were evoked by the voltage-pulse protocol shown. The pipette contained a Cs-glutamate-rich solution (12 mM Cl^-). **A** (*a*) Traces of whole-cell currents obtained from a surface cell surrounding orifice of a crypt. The bath contained a NMDG-Cl-rich solution (147 mM Cl^-). (*b*) Current–voltage (*I–V*) relation for time-dependent current obtained from the cell shown in (*a*). *Inset*: The mean *I–V* relations obtained from 15 different cells. **B** (*a*) Current traces obtained from the same surface cell shown in **A**(*a*) after glutamate substitution for extracellular Cl^-. (*b*) *I–V* relation for the time-dependent current obtained from the cell shown in (*a*). *Inset*: The mean *I–V* relations obtained from 15 different cells. **C** (*a*) Traces of tail currents recorded in control (NMDG-Cl-rich) and test (NMDG-glutamate-rich) solutions from a surface cell surrounding orifice of a crypt. Tail currents were elicited by a hyperpolarizing step pulse to −112 mV (or −106 mV) for 800 ms from a holding potential of −12 mV (or −6 mV), followed by a step pulse from −82 (or −76) to −2 (or +4) mV for 200 ms. (*b*) Tail current amplitudes plotted against tail current voltages in Cl^-- (*solid circles*) or glutamate-rich solution (*open circles*). Data were obtained from the cell shown in (*a*). **D** (*a*) Tail currents recorded from the same surface cell in a NaCl- or NaI-rich bath solution containing amiloride (10 μM). (*b*) Tail current amplitudes plotted against tail current voltages. Data were obtained from the cell shown in (*a*). (*c*) Shift of reversal potential of the tail currents upon Br^-, I^- or glutamate substitution for Cl^- (145 mM) in the bath solution. Values are means ± SE of 3–7 experiments

surface cell surrounding orifice of a crypt, and demonstrates that a slowly activating inward current was observed at a membrane potential more negative than −72 mV. When the time-dependent current amplitude was quantified by subtracting the initial clamp current from the current at the end of the voltage step, the corresponding current–voltage (*I–V*) relation revealed a strong inward rectification (Fig. 1A(b) and inset). The inwardly rectifying current appeared not to be carried by monovalent cations because the bath solution contained no K^+ and Na^+ ions. When external Cl^- concentration was reduced from 147 mM to 2 mM by glutamate substitution, slowly activating currents were evoked even at −46 mV, and the tail currents at −6 mV completely disappeared (Fig. 1B(a) and (b)). The conclusion that the currents were most likely mediated by a Cl^- conductance was strengthened by experiments where the reversal potential of tail currents after current activation was measured by using a step pulse protocol (see also Fig. 1C and D). When the cells were dialyzed with a pipette solution containing 12 mM Cl^- in a bath solution with 147 mM Cl^-, the mean reversal potentials obtained were −58.9 ± 1.6 mV ($n = 18$), the values being closed to the equilibrium potential for Cl^- (E_{Cl}) of −64.3 mV. Similar currents were observed in approximately 90% (132 out of 147 cells) of the cells tested in the whole-cell configuration. The current will hereafter be designated $I_{Cl\text{-}IR}$ in this article.

To characterize electrophysiological properties of $I_{Cl\text{-}IR}$ in detail, its anion selectivity was determined by replacing external Cl^- with other foreign anions (but 2 mM Cl^- was present in the test solution) and by measuring the reversal potential of tail currents after channel activation. The replacement of external NMDG-Cl with NMDG-Br or NMDG-glutamate induced the shift of the reversal potential of +6.3 ± 1.4 mV ($n = 5$) or +47.4 ± 4.0 mV ($n = 9$) (Fig. 1C(a) and (b)), relative permeability ratio corresponding to 0.78 ± 0.05 (P_{Br}/P_{Cl}, $n = 5$) or 0.16 ± 0.03 ($P_{glutamate}/P_{Cl}$, $n = 9$), respectively. Relative permeability ratio for I^- (P_I/P_{Cl}) was also estimated in experiments where external NaCl was totally replaced with NaI in the bath solution. Upon the I^- substitution, the mean changes in reversal potential were +22.3 ± 5.4 mV ($n = 5$), indicating the P_I/P_{Cl} to be 0.45 ± 0.09 ($n = 5$) (Fig. 1D(b) and (c)). We also noted that external I^- reduced an inward current attributable to Cl^- efflux (Fig. 1D(a)), suggesting its blockade of the channel.

Replacement of external NaCl with NaBr or Na-glutamate also caused the shift of the reversal potential of +4.3 ± 2.7 mV ($n = 3$) or +36.0 ± 6.2 mV ($n = 7$) (Fig. 1D(c)), corresponding relative permeability ratio being 0.85 ± 0.10 (P_{Br}/P_{Cl}, $n = 3$) or 0.28 ± 0.07 ($P_{glutamate}/P_{Cl}$, $n = 7$), respectively. These results together indicate that the anion selectivity sequence of $I_{Cl\text{-}IR}$ was $Cl^- > Br^- > I^- >$ glutamate.

We also examined the voltage dependence of the current activation. After stepping from a holding potential (−12 mV) to various test voltages, current activation was monitored at a constant "tail" voltage (−12 mV) (Fig. 2A(a)). Figure 2A(b) summarizes the plot of the tail currents at −12 mV normalized to the current after a prepulse of −92 mV against the test prepulse voltages. The normalized current amplitude at −32, −52, −72, and −112 mV were 0.25 ± 0.03 ($n = 14$), 0.33 ± 0.03 ($n = 14$), 0.52 ± 0.03 ($n = 14$), and 1.66 ± 0.07 ($n = 9$), respectively, suggesting that gating of the native channel was activated by membrane hyperpolarization. The time-dependent activation was also analyzed by fitting current activation to Eq. 1 (See Materials and Methods). Figure 2B(a) shows current traces obtained from a surface cell surrounding orifice of a crypt (together with the fitted lines), indicating that time course of activation can be best described by single or double exponential components with time constants (τ), which were 295.8 ms at −82 mV, 47.9 and 184.0 ms at −102 mV, and 21.2 and 79.0 ms at −122 mV, respectively. The time constants were voltage dependent and became faster with membrane hyperpolarization, so that mean time constants (τ_1 and τ_2) at −112, −132 or −152 mV were 39.0 ± 5.1 ms ($n = 13$) and 178.6 ± 22.3 ms ($n = 15$), 28.3 ± 5.6 ms ($n = 8$) and 105.3 ± 22.6 ms ($n = 9$), or 13.3 ± 1.9 ms ($n = 10$) and 85.1 ± 24.8 ms ($n = 10$), respectively (Fig. 2B(b)).

We examined the effect of external Zn^{2+} on $I_{Cl\text{-}IR}$ (Fig. 2C). In these experiments, we used a NMDG-Cl-rich pipette solution ($Cl^- = 132$ mM) especially to test its inhibitory action at a membrane potential between −40 and −80 mV (a physiological range of resting membrane potential). Figure 2C(a) demonstrates that external Zn^{2+} (0.1 mM) inhibits $I_{Cl\text{-}IR}$. Zn^{2+} (0.1 mM) reduced the current by 68.1 ± 12.3% ($n = 4$), 46.9 ± 11.2% ($n = 4$), 48.4 ± 12.6% ($n = 4$) and 35.4 ± 12.0% ($n = 4$) at −60, −80, −100, and −120 mV, respectively (Fig. 2C(b):inset). Zn^{2+} were likely more effective in inhibiting the currents with less membrane hyperpolarization (Fig. 2C(b) and inset) as reported for a native ClC-2-like Cl^- current in dissociated rat sympathetic neurons (Clark et al. 1998). The inhibition was pronounced by adding a higher concentration of Zn^{2+} (1 mM) to either a NMDG-Cl-rich or a NaCl-rich standard solution, such that the current was inhibited by 94.4 ± 5.6% ($n = 6$) at −40 or −43 mV or 80.4 ± 5.5% ($n = 6$) at −120 or −123 mV, respectively (Fig. 2C(b):inset).

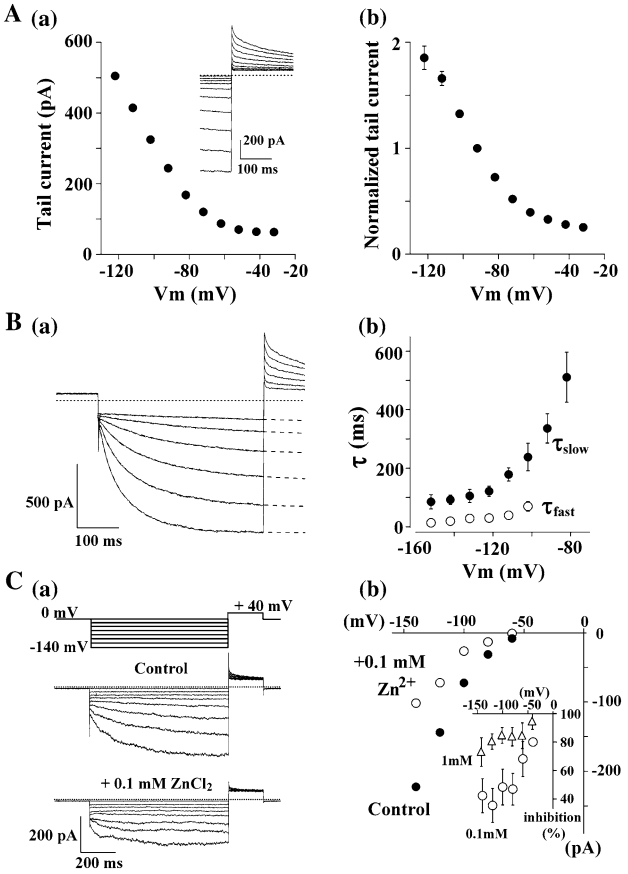

Fig. 2 Biophysical and pharmacological properties of native $I_{Cl\text{-}IR}$ currents. **A** (*a*) The tail current amplitudes plotted against the test pulse voltages. Data were from the cell shown in inset. *Inset*: Traces of whole-cell currents evoked by the pulse protocol using the pipette and bath solutions as described in Fig. 1A. For the illustration purposes, a part of the traces was deleted. (*b*) Summary of the voltage-dependent activation of gating. Values are means ± SE of 4–14 experiments. **B** (*a*) Time-dependent current activation. Current traces at −72, −82, −92, −102, −112, and −122 mV are shown. (*b*) Plot of exponential time constants (τ_{fast} and τ_{slow}) for two components of current activation against membrane potentials. Values are means ± SE of 6–15 experiments. **C** (*a*) Currents recorded from an isolated cell that was likely dissociated from surface epithelium of crypt before (*middle*) and after (*bottom*) addition of 0.1 mM Zn^{2+} to the NMDG-Cl-rich bath solution. (*b*) Current–voltage relations for time-dependent currents obtained from the cell shown in (*a*) in the absence (*solid circles*) and presence of 0.1 mM Zn^{2+} (*open circles*) in the bath solution. *Inset*: Summary of the effect of 0.1 and 1 mM Zn^{2+} at different membrane potentials. In two experiments, 1 mM Zn^{2+} was also tested in a NaCl-rich bath solution, and the data were also included in the figure. Values are means ± SE of 3–6 experiments

In a previous study, we showed that surface epithelial cells of rat rectal colon exhibited an amiloride-sensitive ENaC current in the standard whole-cell mode (with a Cs-glutamate-rich pipette solution), where the incidence of ENaC currents was found to be approximately 20% of the cells tested (Inagaki et al. 2004a). Thus, we also have

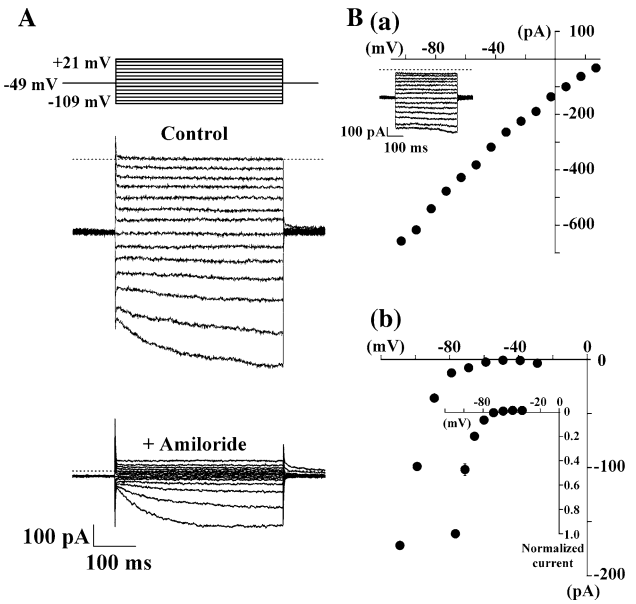

Fig. 3 Functional coexpression of ENaC and ClC-2-like currents in surface epithelial cells of rat rectal colon. **A** Whole-cell currents recorded from a surface cell surrounding orifice of a crypt in the absence (control) or presence of external amiloride (10 μM). The bath contained the standard NaCl-rich solution (154 mM Cl^-). **B** (*a*) *I–V* relation for amiloride-sensitive whole-cell currents recorded from the cell shown in (**A**). *Inset*: Traces of amiloride-sensitive currents obtained from the traces in the absence and presence of amiloride shown in (**A**). (*b*) *I–V* relation of time-dependent, amiloride-insensitive currents recorded from the cell shown in (**A**) (*bottom*). *Inset*: Summary of *I–V* relations of ClC-2-like currents obtained from surface cells expressing amiloride-sensitive currents. Time-dependent current amplitudes were normalized to the value at −109 mV. Values are means ± SE of 4 experiments

examined whether both ENaC and $I_{Cl\text{-}IR}$ currents would be coexpressed in the same surface cells. Figure 3A shows traces of whole-cell currents recorded from a surface cell surrounding orifice of a crypt. The cell was dialyzed with a Cs-glutamate-rich solution containing 12 mM Cl^- in a NaCl-rich bath solution. It was apparent that two types of current were evoked by voltage steps between −109 and +21 mV from the holding potential of −49 mV (Fig. 3A, upper traces). One activated in a range of voltages studied, displayed little, if any, time dependence, and was inhibited by external amiloride (10 μM) (Fig. 3B(a) and inset). Another component, which was mediated by $I_{Cl\text{-}IR}$ was observed at a voltage more negative than −79 mV and became much clearer when amiloride (10 μM) was added to the bath solution (Fig. 3A, lower traces and Fig. 3B(b)). Intriguingly, the surface cells expressing ENaC currents ($n = 12$) consistently exhibited an inwardly rectifying Cl^- current under the present experimental conditions (i.e., using a low Cl^- pipette solution). $I_{Cl\text{-}IR}$ amplitudes in surface cells exhibiting ENaC currents were indistinguishable from those with no ENaC currents, so that they were −144.6 ± 54.3 pA ($n = 4$) and −159.5 ± 30.2 pA ($n = 11$) at −109 mV, respectively (holding potential: −9 mV or −49 mV; the bath solution: NaCl + 10 μM amiloride) ($P = 0.81$).

In Situ Hybridization and Immunohistochemical Analysis of ClC-2 in Rat Rectal Colonic Epithelium

We next investigated molecular expression of rClC-2 in the rat rectal surface cells. RT-PCR analysis showed that the

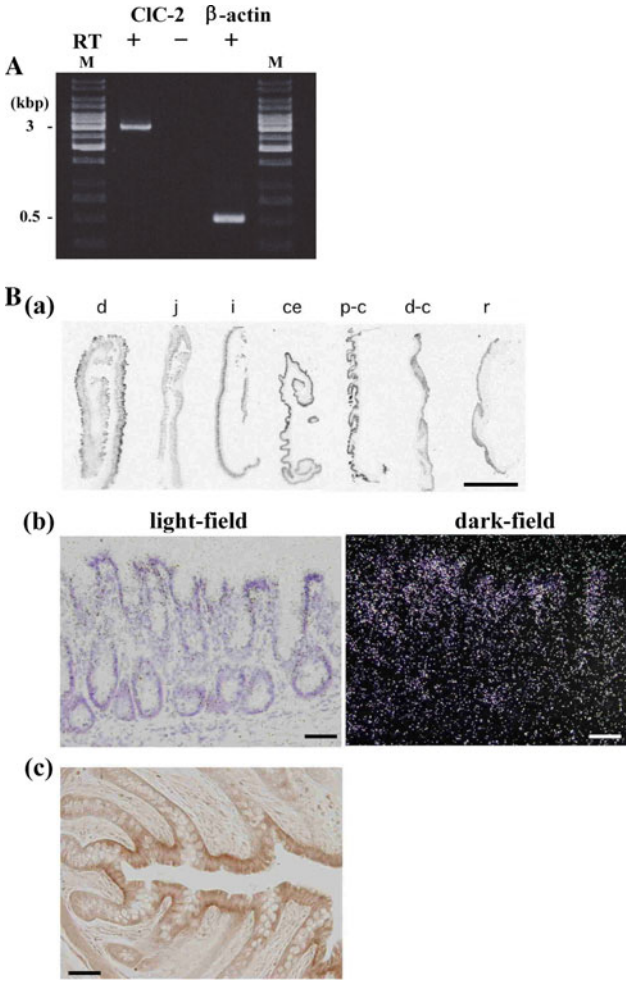

Fig. 4 Molecular expression of rClC-2 in rectal surface cells. **A** RT-PCR analysis of rClC-2 in a rectal colonic mucosa. PCR products were resolved by 1% agarose gel electrophoresis, and an amplicon (rClC-2, 2935 bp) was detected by staining with ethidium bromide. As a control, *β*-actin cDNA (510 bp) was amplified. No DNA fragment was amplified with the template without RT treatment. M, size markers (stable 1 kb DNA ladder, Sigma Genosys, Japan). **B** (*a*) X-ray film image showing mRNA expression of rClC-2 throughout the intestine. The mRNA is extensively present from the duodenum (d) to the rectum (r), except the jejunum (j). i, ileum; ce, cecum; p-c, proximal colon; d-c, distal colon. Bar, 5 mm. (*b*) Light micrographs of hybridized sections (light-field and dark-field images of the same area) show accumulations of silver grains for mRNA expression along the surface epithelium and upper part of crypts in the rectum. Bars, 50 μm (*c*) The immunoreactivity for rClC-2 is confined to the surface area of the rectal mucosa. Bar, 50 μm

rectal mucosa expressed the rClC-2 transcript (Fig. 4A). On the basis of the complete sequence information (NM_017137) of the rat ClC-2, we amplified from mRNA two overlapping PCR fragments by RT-PCR with a high fidelity DNA polymerase (Pfu-Turbo), and sequence analysis showed the 100% identity to the rClC-2. By in situ hybridization analysis, significant expression of rClC-2 mRNA was detected in the epithelium along the entire length of the small and large intestine (Fig. 4B(a)). The signals in the small intestine tended to accumulate at villous tips in the duodenum and at the lower part of villi in the ileum, while the expression in the jejunum was less intense. In the large intestine, the signals were much enhanced in the cecum and the proximal colon, but still significant in the distal part of the large intestine. The signals were mostly confined to the surface epithelium of the mucosa and the upper part of crypts in the rectum (Fig. 4B(b)). Corresponding regions in the rectal epithelium were immunoreactive for rClC-2 protein in parallel with the gene expression (Fig. 4B(b)). The immunoreactivity appeared to be diffusely distributed in the cytoplasm of enterocytes with an increased labeling in the basal cytoplasm. Goblet cells, lamina propria cells and smooth muscle were free from the immunoreactivity.

Comparison of Electrophysiological Properties of the Native Currents with Those of rClC-2 Cloned from Rat Rectal Colon

We also compared the electrophysiological properties of recombinant rClC-2 currents expressed in HEK293 cells with those of the native currents under the same ionic conditions. Figure 5A and B shows the current traces obtained from a rClC-2-expressing HEK293 cell bathed in a Cl^-- or glutamate-rich solution and the corresponding *I–V* relation, respectively. The expressed rClC-2 current had an anion permeability sequence of Cl^- (1 by definition: $n = 22$) > Br^- (0.74 ± 0.02; $n = 8$) > I^- (0.15 ± 0.01; $n = 7$) > glutamate (0.07 ± 0.01; $n = 17$) (Fig. 5C(c)), which was consistent with the corresponding sequence for the native current. In these experiments, we also observed a block by external Br^- or I^- of the time-dependent inward current attributable to Cl^- efflux (Fig. 5C(a)). When the tail current amplitudes at −12 mV normalized to the current after a prepulse of −192 mV were plotted as a function of the test prepulse voltages, they could be fitted to Boltzmann distributions (Eq. 2, See "Materials and Methods") (Fig. 5D with a $V_{0.5}$ value of -133.1 ± 4.2 mV ($n = 11$) and a k value of 23.5 ± 1.0 mV ($n = 11$)). When external Cl^- concentration was reduced from 147 to 2 mM by glutamate substitution, *I–V* relation shifted toward positive membrane potential (Fig. 5B and D), similar to what was observed for native currents (see Fig. 1A and B). Subsequent experiments showed that the Cl^- replacement with glutamate caused a change of $V_{0.5}$, so that the mean values were estimated to be -92.2 ± 4.0 mV ($n = 6$), which was significantly different from those obtained in a Cl^- rich bath solution ($P = 0.000012$ (Fig. 5D)). Time course of current activation could be described by one or two components, which were becoming faster with membrane hyperpolarization. Mean time constants (τ_1 and τ_2) at −112, −132 or −152 mV were 78.5 ± 29.1 ms ($n = 6$) and 517.0 ± 65.2 ms ($n = 14$), 47.4 ± 7.0 ms ($n = 13$) and 274.2 ± 43.5 ms ($n = 14$) or 30.0 ± 5.8 ms ($n = 14$) and 175.4 ± 32.7 ms ($n = 14$), respectively (Fig. 5E). We also confirmed that the voltage-dependent gating is affected by the intracellular Cl^- concentration, so that $V_{0.5}$ values were -116.9 ± 3.9 mV ($n = 15$), -108.7 ± 4.3 mV ($n = 9$), and -80.6 ± 8.2 mV ($n = 5$) at 32, 72 and 132 mM, respectively (Fig. 5F). 0.1 and 1 mM Zn^{2+} inhibited the expressed currents at −40 and −120 mV by $58.2 \pm 14.6\%$ ($n = 4$) and $75.6 \pm 18.7\%$ ($n = 4$), and $23.5 \pm 7.5\%$ ($n = 4$) and $79.4 \pm 6.1\%$ ($n = 4$), respectively (Fig. 5G(a), (b) and (c)). As observed in native surface cells, the block was voltage dependent (Fig. 5G(b) and (c)), so that a lower concentration of Zn^{2+} (0.1 mM) reduced the rClC-2 currents by $52.0 \pm 4.5\%$ ($n = 4$), $40.2 \pm 6.7\%$ ($n = 4$), $28.5 \pm 6.8\%$ ($n = 4$) at −60, −80, and −100 mV, respectively.

Hyperpolarization-Activated, Inwardly Rectifying Currents in Cell-attached Patches on Surface Epithelial Cells

The experiments described so far suggested that rat surface epithelial cells exhibited an inwardly rectifying Cl^- conductance, which was most likely mediated by rClC-2. Given a strong voltage-dependent activation of the native Cl^- currents, however, it remained unclear whether the ClC-2-like current would activate at resting membrane potential in intact (i.e., nondialyzed) surface cells. To address this issue, we performed cell-attached patch experiments on surface epithelial cells surrounding orifices of crypts acutely dissociated from rectal colon of rats fed a standard diet. The pipette solution was rich in NMDG to prevent an inward current attributable to cation influx across the patch membrane, and the bath was the standard NaCl-rich solution. Under these experimental conditions, we first confirmed in HEK293 cells expressing rClC-2 that a slowly activating inward current could be observed in cell-attached patch mode (12 out of 27 cells tested) and its *I–V* relation revealed a strong inward rectification (Fig. 6A and B). Some successful inside-out patch experiments also showed that the currents were mainly carried by Cl^-, because replacement of cytosolic Cl^- with glutamate markedly reduced the time-dependent inward current

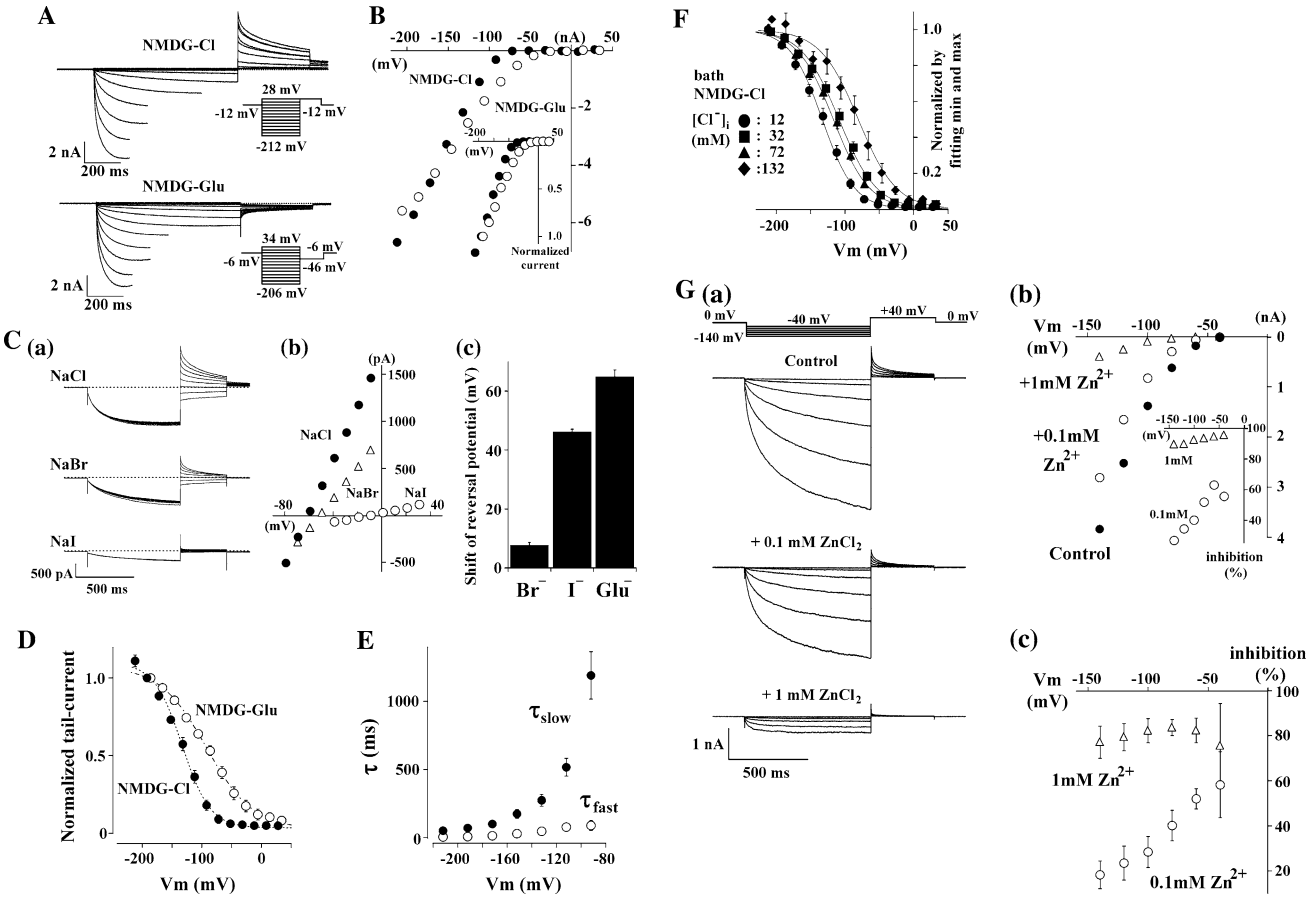

Fig. 5 Electrophysiological properties of heterologously expressed rClC-2 currents. **A** Whole-cell currents recorded from a HEK293 cell stably transfected with rClC-2 cloned from rat rectal mucosa. When the cells were dialyzed with the pipette solution having 12 mM Cl^-, the rClC-2 current evoked by a strong membrane hyperpolarization (usually more negative than −152 mV) reached a maximal level and then gradually decreased, similar to what has been also observed in native surface cells (not shown). A comparable phenomenon has been also noted for rClC-2 previously (Varela et al. 2002). Therefore, the duration of the test pulses was decreased at more negative voltages, where current activation had a faster time course. For the illustration purposes, the beginning of the tail currents at +28 mV (or −46 mV) was set at the same time. Pipette and bath solutions were Cs-glutamate rich (12 mM Cl^-) and NMDG-Cl rich (147 mM Cl^-) (*top*) or NMDG-glutamate-rich (2 mM Cl^-) (*bottom*), respectively. **B** Corresponding *I–V* relations for the time-dependent currents obtained from the cell shown in (**A**). *Inset*: The mean *I–V* relations. Time-dependent current amplitudes were normalized to the value at −192 mV or −186 mV, respectively. Values are means ± SE of 4–6 experiments. Error bars smaller than symbols are not shown. **C** (*a*) Current traces obtained from a HEK293 cell expressing rClC-2 in a NaCl-rich, NaBr-rich, or NaI-rich solution. Currents were elicited by a hyperpolarizing step pulse to −109 mV for 800 ms from a holding potential of −49 mV, followed by a step pulse between −79 (−69, or −39) and −9 (or +31) mV for 400 ms and by a pulse to −49 mV. Pipette solution was Cs-glutamate rich (12 mM Cl^-). (*b*) Tail current amplitudes plotted against tail current voltages in solution rich in Cl^- (*solid circles*), Br^- (*open triangles*), or I^- (*open circles*). Data were obtained from the same cell shown in (*a*). (*c*) Shift of reversal potential of the tail currents upon Br^-, I^-, or glutamate substitution for external Cl^- (145 mM). Values are means ± SE of 7–17 experiments. **D** Tail current amplitudes normalized to that at −192 (or −186) mV plotted against the test pulse voltages. The tail current amplitudes were measured at the beginning of a pulse to −12 (or −46) mV. Pipette and bath solutions were rich in Cs-glutamate (12 mM Cl^-) and NMDG-Cl (147 mM Cl^-) (*solid circles*) or NMDG-glutamate (2 mM Cl^-) (*open circles*), respectively. Values are means ± SE of 6–11 experiments. **E** Plot of exponential time constants (τ_{fast} and τ_{slow}) for two components of current activation against membrane potentials. Pipette and bath solutions were rich in Cs-glutamate (12 mM Cl^-) and NMDG-Cl (147 mM Cl^-), respectively. Values are means ± SE of 4–14 experiments. **F** Effect of cytosolic Cl^- concentrations on rClC-2 currents. The bath solution was NMDG-Cl rich. The pulse protocol was similar to that described in (**D**). Tail current amplitude as a function of membrane potential was fit to Eq. 2 (see "Materials and Methods"), and then each value was normalized to estimated minimum and maximum. **G** (*a*) Recombinant rClC-2 currents obtained from a HEK293 in a NMDG-Cl-rich solution in the absence (control) and the presence of 0.1 or 1 mM Zn^{2+}. The pipette solution was NMDG-Cl rich. (*b*) *I–V* relations for time-dependent currents obtained from the cell shown in (*a*) in the absence (*solid circles*) and the presence of 0.1 mM (*open circles*) or 1 mM Zn^{2+} (*open triangles*) in the bath solution. *Inset*: Inhibitory effects of 0.1 mM (*open circles*) or 1 mM Zn^{2+} (*open triangles*) at different membrane potentials. (*c*) Summary of the inhibitory effects of 0.1 mM (*open circles*) or 1 mM Zn^{2+} (*open triangles*) at different membrane potentials. Values are means ± SE of 4 experiments

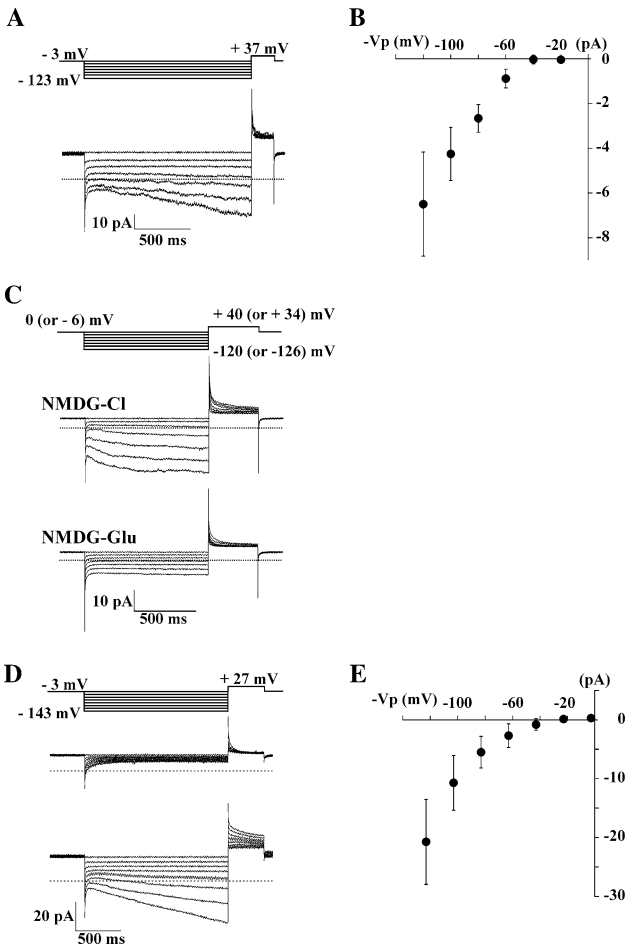

Fig. 6 Slowly developing, hyperpolarization-activated inward currents in cell-attached patches. **A** Traces of slowly developing, hyperpolarization-activated inward currents in cell-attached patch obtained from a HEK293 cell transfected with rClC-2. **B** The mean *I–V* relations of the time-dependent components in cell-attached patches on HEK293 cells. Values are means ± SE of 7–8 experiments. Vp, pipette potential. **C** Traces of slowly developing, hyperpolarization-activated inward currents in an excised inside-out patch obtained from a HEK293 cell transfected with rClC-2. The bath solution was NMDG-Cl or NMDG-glutamate rich and contained 10 mM EGTA. **D** *Middle*: Traces obtained from a cell-attached patch obtained from a surface epithelial cell surrounding orifice of a crypt, which did not exhibit slowly developing, hyperpolarization-activated currents. *Bottom*: Traces of slowly developing, hyperpolarization-activated currents in a cell-attached patch obtained from a surface epithelial cell surrounding orifice of a crypt. **E** The mean *I–V* relations of the time-dependent components in cell-attached patches on native surface epithelial cells. Values are means ± SE of 7–8 experiments

(Fig. 6C). Figure 6D shows traces of currents recorded from cell-attached patches on two different surface cells surrounding orifices of crypts and demonstrates that a time-dependent, inwardly rectifying current could be observed, but only elicited by strong hyperpolarization of the membrane patch (Fig. 6D, lower traces). Summary of *I–V* relations obtained from 7–8 cells in the same experimental condition is also shown in Fig. 6E and suggests that the native ClC-2-like currents activate only at potentials at least 40 mV more negative than resting potentials. In 14 out of 21 cells tested under similar but not identical experimental conditions, comparable currents were observed.

Effects of Zn^{2+} on Basal Amiloride-Sensitive I_{sc} in Rat Rectal Mucosa

Cell-attached patch experiments provided no evidence for the current activation at resting membrane potential in intact rat rectal surface cells. We finally examined if pharmacological inhibition of ClC-2-like currents would affect basal electrogenic Na^+ transport in rectal mucosa of rats fed a normal-salt diet. Because ClC-2-like channel activity would depolarize the membrane potential toward E_{Cl}, and thereby decreasing amiloride-sensitive short-circuit current ($I_{sc\text{-}amil}$), one can predict that its inhibition could increase $I_{sc\text{-}amil}$. We therefore tested the effect of Zn^{2+}, which inhibited $I_{Cl\text{-}IR}$ and rClC-2 currents (Figs. 2 and 5) on basal $I_{sc\text{-}amil}$ in rat rectal mucosa mounted in Ussing-type chambers. We first confirmed the previous observations that the rectal mucosa exhibited $I_{sc\text{-}amil}$ under basal conditions (Inagaki et al. 2004a). As shown in Fig. 7A(a), when amiloride (10 μM) was added to the apical solution during two consecutive periods, the responses to the drug were comparable, so that the first and second $I_{sc\text{-}amil}$ were 29.3 ± 4.5 μA/cm^2 and 26.2 ± 4.3 μA/cm^2 ($n = 11$), respectively (Fig. 7A(b)). Such fairly stable and reproducible responses to amiloride allowed us to ensure that basal $I_{sc\text{-}amil}$ was comparable and to examine the effect of Zn^{2+} on the second $I_{sc\text{-}amil}$ in different mucosal preparations (Fig. 7A(b)). We subsequently examined whether basolateral application of Zn^{2+} (0.1 mM) would affect basal $I_{sc\text{-}amil}$ (Fig. 7B(a) and (b)). However, there was little, if any, effects of Zn^{2+} (Fig. 7B(a) and (b)). In these experiments, the first $I_{sc\text{-}amil}$ (29.2 ± 3.1 μA/cm^2, $n = 7$) were similar to those observed in control experiments (29.3 ± 4.5 μA/cm^2, $n = 11$) ($P = 0.99$). The second $I_{sc\text{-}amil}$ values in the presence of basolateral Zn^{2+} (0.1 mM) were 30.9 ± 2.5 μA/cm^2 ($n = 7$), which were not significantly different from the corresponding values in control experiments (26.2 ± 4.3 μA/cm^2 ($n = 11$)) ($P = 0.43$) either (Fig. 7A(b) and B(b)), although the second $I_{sc\text{-}amil}$ (108.4 ± 5.5%, $n = 7$) normalized to the first one (100% by definition) was slightly, but significantly larger than the corresponding value (90.3 ± 4.6%, $n = 11$) in the control experiments ($P = 0.02$). Apical Zn^{2+} (0.1 mM) had no effects on basal $I_{sc\text{-}amil}$, so that the first (27.1 ± 5.3 μA/cm^2, $n = 4$) and second $I_{sc\text{-}amil}$ values (27.0 ± 5.7 μA/cm^2, $n = 4$) were not different from the corresponding control values ($P = 0.79$ and $P = 0.93$, respectively) (Fig. 7C).

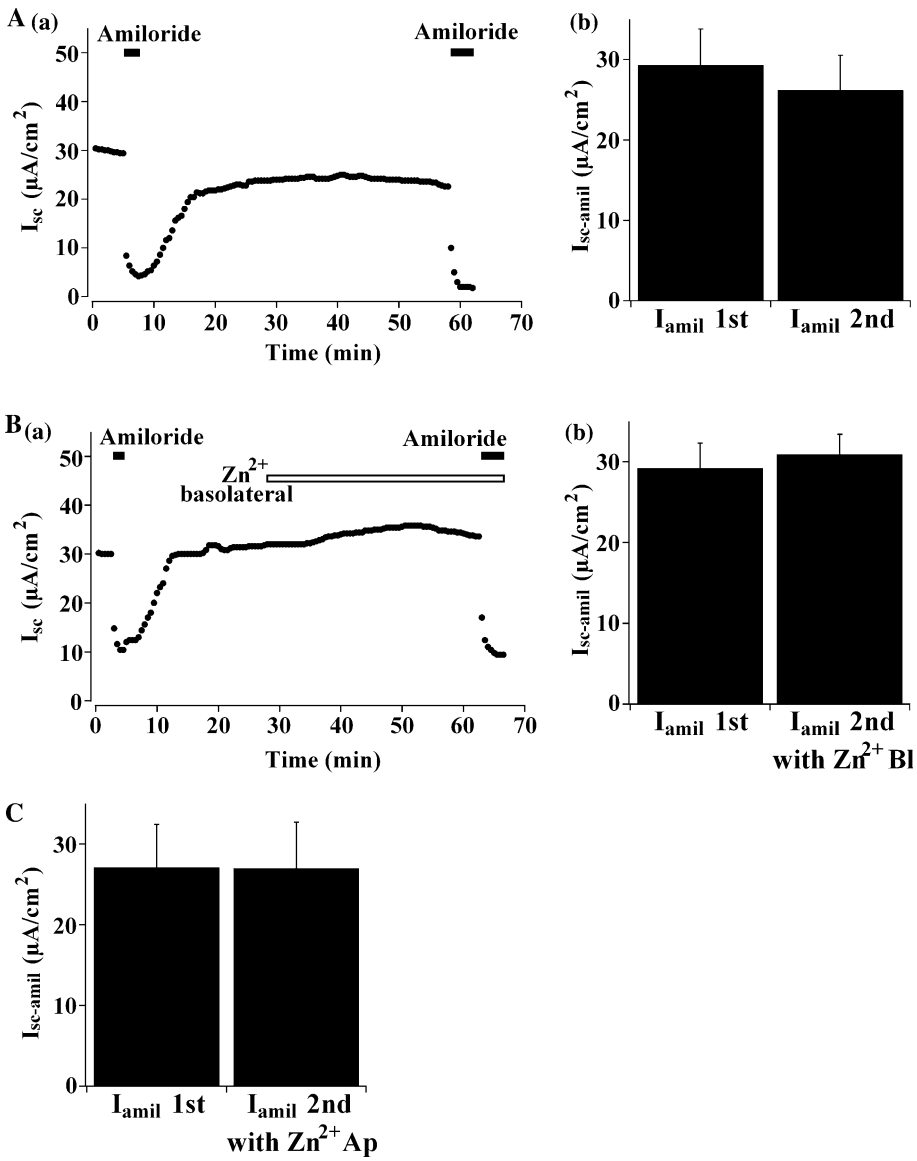

Fig. 7 Effects of Zn^{2+} on amiloride-sensitive I_{sc} of the rectal colonic mucosa. **A** Effects of amiloride (10 μM) on basal I_{sc} in rectal mucosa. (*a*) An example of the control experiments. A positive deflection of I_{sc} indicates cation movement from apical to basolateral bathing medium or anion movement from basolateral to apical medium. (*b*) Summary of amiloride-sensitive I_{sc} ($I_{sc\text{-}amil}$) in experiments as shown in (*a*). Values are means ± SE of 11 experiments. **B** Effects of basolateral Zn^{2+} on $I_{sc\text{-}amil}$ under basal conditions. (*a*) After control $I_{sc\text{-}amil}$ was evaluated, 0.1 mM Zn^{2+} was added to the basolateral solution 35 min before the second addition of 10 μM amiloride to the apical solution. (*b*) Summary of the effects of basolateral Zn^{2+} (0.1 mM) on basal $I_{sc\text{-}amil}$. Values are means ± SE of 7 experiments. **C** Effects of apical Zn^{2+} on $I_{sc\text{-}amil}$ under basal conditions. Values are means ± SE of 4 experiments

Discussion

Previous immunohistochemical studies showed that ClC-2 is expressed in surface epithelial cells of the distal colon, at least in humans, rats, guinea pigs, and mice (Catalán et al. 2002; Lipecka et al. 2002; Peña-Münzenmayer et al. 2005). However, direct electrophysiological evidence for its functional expression at the surface cell level has been lacking in most species except guinea pigs (Catalán et al. 2002, 2004). Here, we have provided several lines of evidence for the expression of a ClC-2-like conductance in rat rectal surface cells. First, in situ hybridization experiments showed expression of ClC-2 mRNA in rat rectal surface epithelial cells. In line with this finding, ClC-2 immunoreactivity was also observed in these cells, although there was diffuse immunostaining over the cytosolic compartment. Second, whole-cell patch clamp studies revealed a slowly activating, inwardly rectifying Cl^- current ($I_{Cl\text{-}IR}$), which also shared several common electrophysiological properties with the rClC-2 currents heterologously expressed in HEK293 cells under similar experimental conditions: (1) an anion permeability sequence of $Cl^- > Br^- > I^-$ > glutamate, (2) inhibition of the inward current by an external halide anion such as Br^- and I^-, (3) voltage-dependent activation of gating, and (4) voltage-dependent inhibition by external Zn^{2+}. Although we have not systematically characterized the intracellular Cl^- ($[Cl^-]_i$) dependence of the native channel gating, activation by voltage appeared to saturate at more positive potentials in 132 mM than 12 mM $[Cl^-]_i$ (e.g., see Fig. 2A(a) and C(a) upper trace). Such a $[Cl^-]_i$-dependent gating appears to be similar to that reported for the cloned rClC-2 heterologously expressed in mammalian cells (Hinzpeter et al. 2006; Fig. 5F). Moreover, both native and rClC-2 currents

apparently activated at less negative voltages, when extracellular Cl^- concentration ($[Cl^-]_o$) was decreased to 2 mM by replacement with glutamate, a much less permeable anion. In fact, the glutamate substitution caused a shift in $V_{0.5}$ for the activation of rClC-2 current toward positive membrane potential. A comparable phenomenon has been reported for rClC-2 expressed in *Xenopus* oocytes and interpreted as indicating that binding of extracellular Cl^- favors a closed state (Pusch et al. 1999).

Besides these similarities of both native and recombinant currents, the kinetics of the native current seemed to be faster than that of rClC-2 current, although activation time courses of both currents were mainly described by two components, for which exponential time constants were also voltage dependent. The reason for the discrepancy is unclear at present. It might be due to the different cellular environments, where the channel is expressed, because ClC-2 gating kinetics is shown to be modulated by membrane cholesterol content, which appears to depend on cell types, and metabolic and oxidative states of the cells (Hinzpeter et al. 2007). We cannot completely exclude the possibility that the native currents might be mediated by splice variants of ClC-2 as shown in guinea pig distal colon (Cid et al. 2000), although activation kinetics of native currents from guinea pig surface cells was comparable to those of inwardly rectifying Cl^- currents generated by these variants (Cid et al. 2000; Catalán et al. 2002). Further experiments will be necessary to address these issues.

rClC-2 was originally characterized to be mostly shut down under resting conditions in *Xenopus* oocyte heterologous expression system (Thiemann et al. 1992). Accordingly, an important question concerns as to whether the magnitude of the native ClC-2-like conductance is sufficient to contribute largely to cellular conductance and thus to electrogenic Na^+ absorption of rat rectal surface cells under basal physiological conditions. Some observations in the present study may give a clue to this issue. First, tail current analysis in the whole-cell patch-clamp experiments suggested that apparent open probability (P_o) of the channel was likely to be very low at around −40 and −50 mV (Fig. 2A(b)), a membrane potential being reported for surface cells of distal colon of rats fed a normal or a Na^+-depleted diet (Lomax et al. 1994) and of rats treated with or without dexamethasone (Ecke et al. 1996). Even assuming that P_o of the native ClC-2-like channel is regulated by cytosolic Cl^- concentration as well as the heterologously expressed ClC-2 channel (Pusch et al. 1999; Catalán et al. 2004; Hinzpeter et al. 2006, this study), the value would be still low in the presence of a higher cytosolic concentration of Cl^- (e.g., 32 mM): P_o of heterologously expressed rClC-2 is estimated to be only 0.052 ± 0.007 ($n = 16$) at −51 mV (Fig. 5F). Furthermore, even when the native surface cells were dialyzed with a very high Cl^- pipette solution ($Cl^- = 132$ mM), the $I_{Cl\text{-}IR}$ amplitudes were -4.7 ± 1.6 pA and -33.5 ± 6.9 pA ($n = 9$) at −40 and −60 mV, respectively (Fig. 2C), and they would give a cellular ClC-2-like conductance of an approximately 1.4 nS/cell, for which a driving force of 10 mV would be required to allow a net inward current of 14 pA/cell. Thus, one can expect that much larger driving force than 10 mV would be required for the same order of the currents or that the same order of the driving force would only allow much smaller current than 14 pA/cell at physiological intracellular Cl^- concentrations. Second, although ClC-2-like currents were elicited in cell-attached mode (i.e., in nondialyzed intact surface cells), the currents activated only on a very strong membrane hyperpolarization, suggesting that the channel may not conduct sufficient inward Cl^- current in unstimulated surface cells, at least under the present experimental conditions. Finally, Ussing chamber experiments showed that neither basolateral nor apical application of Zn^{2+} (0.1 mM), which inhibited both rClC-2 and native currents, had major effects on basal $I_{sc\text{-}amil}$. Therefore, at this stage, it appears to be safe to conclude that the channel activity may not be essential, at least, for controlling the basal electrogenic Na^+ transport in rat rectal colon, likely as a result of its minimal activity and/or contribution to the cellular conductance under quasi-physiological conditions.

It should be stressed that our data do not exclude the possibility that the channel is activated under other physiological and pathophysiological conditions. Heterologously expressed rClC-2 currents are reported to be activated by cell swelling (hypo-osmotic shock) (Gründer et al. 1992; Xiong et al. 1999). Although a basolateral Cl^- conductance in rat distal colonic epithelium is also shown to be activated during cell swelling (Diener et al. 1992), the underlying Cl^- channel is probably not ClC-2, because *I–V* relation of the conductance is outwardly rectifying and the single channel conductance is 20–30 pS (Diener et al. 1989, 1992), both of which seem to be clearly different from those for the native (Nobile et al. 2000) and cloned rat ClC-2 channels (Weinreich and Jentsch 2001). In principle, basolateral Cl^- channels are expected not only to facilitate transepithelial Cl^- absorption, but also to impede the transepithelial Cl^- secretion. In view of this, it is interesting to note that I_{sc} component of distal colonic epithelium attributable to electrogenic Cl^- secretion induced by a moderate concentration of forskolin (1 μM), but not a higher one (10 μM), was significantly larger in ClC-2 KO mice than in control mice fed on a low Na^+ diet (Zdebik et al. 2004). These observations may imply that the basolateral ClC-2 might be activated under particular cAMP-related condition in native colonic epithelial cells, although cAMP-dependent protein phosphorylation of rClC-2 is shown to be independent of the channel activity (Park et al.

1998). Extracellular proton is also suggested to be a major regulatory factor of ClC-2 gating (Arreola et al. 2002; Niemeyer et al. 2009), and thus the channel, especially at the basolateral membrane, might be activated under particular physiological conditions (e.g., during absorption of short-chain fatty acids), where significant acidic shifts in extracellular pH might occur. Finally, increasing evidence suggests that energy states of the cells may modulate overall ClC-2 activities. It has been shown that adenosine triphosphate (ATP) depletion increases overall activity of ClC-2 by changing its gating properties (Niemeyer et al. 2004) and cell surface expression (Dhani et al. 2008) and that ClC-2 in apical tight junctions may mediate restoration of mucosal barrier function in ischemia-injured porcine ileum via Cl^- secretion (Moeser et al. 2004). Further studies are required to examine whether the native ClC-2-like channel becomes active enough to contribute significantly to the cellular conductance and thus functions of colonic surface cells under the conditions mentioned above.

Acknowledgments This study was supported in part by the Akiyama Foundation and the Suzuken Memorial Foundation.

References

Arreola J, Begenisich T, Melvin JE (2002) Conformation-dependent regulation of inward rectifier chloride channel gating by extracellular protons. J Physiol 541:103–112

Bachhuber T, Almaca J, Aldehni F, Mehta A, Amaral MD, Schreiber R, Kunzelmann K (2008) Regulation of the epithelial Na^+ channel by the protein kinase CK2. J Biol Chem 283:13225–13232

Binder HJ, Sandle GI (1994) Electrolyte transport in the mammalian colon. In: Johnson LR, Alpers DH, Christensen J, Jacobson ED, Walsh JH (eds) Physiology of the gastrointestinal tract. Raven Press, New York, pp 2133–2171

Bösl MR, Stein V, Hübner C, Zdebik AA, Jordt SE, Mukhopadhyay AK, Davidoff MS, Holstein AF, Jentsch TJ (2001) Male germ cells and photoreceptors, both dependent on close cell–cell interactions, degenerate upon ClC-2 Cl^- channel disruption. EMBO J 20:1289–1299

Catalán M, Cornejo I, Figueroa CD, Niemeyer MI, Sepúlveda FV, Cid LP (2002) ClC-2 in guinea pig colon: mRNA, immunolabeling, and functional evidence for surface epithelium localization. Am J Physiol Gastrointest Liver Physiol 283:G1004–G1013

Catalán M, Niemeyer MI, Cid LP, Sepúlveda FV (2004) Basolateral ClC-2 chloride channels in surface colon epithelium: regulation by a direct effect of intracellular chloride. Gastroenterology 126:1104–1114

Cid LP, Niemeyer MI, Ramirez A, Sepúlveda FV (2000) Splice variants of a ClC-2 chloride channel with differing functional characteristics. Am J Physiol Cell Physiol 279:C1198–C1210

Clark S, Jordt SE, Jentsch TJ, Mathie A (1998) Characterization of the hyperpolarization-activated chloride current in dissociated rat sympathetic neurons. J Physiol 506:665–678

Clauss W, Durr J, Rechkemmer G (1985) Characterization of conductive pathways in guinea pig distal colon in vitro. Am J Physiol 248:G176–G183

Dhani SU, Kim Chiaw P, Huan LJ, Bear CE (2008) ATP depletion inhibits the endocytosis of ClC-2. J Cell Physiol 214:273–280

Diener M, Rummel W, Mestres P, Lindemann B (1989) Single chloride channels in colon mucosa and isolated colonic enterocytes of the rat. J Membr Biol 108:21–30

Diener M, Nobles M, Rummel W (1992) Activation of basolateral Cl^- channels in the rat colonic epithelium during regulatory volume decrease. Pflügers Arch 421:530–538

Dinudom A, Young JA, Cook DI (1993) Na^+ and Cl^- conductances are controlled by cytosolic Cl^- concentration in the intralobular duct cells of mouse mandibular glands. J Membr Biol 135:289–295

Ecke D, Bleich M, Schwartz B, Fraser G, Greger R (1996) The ion conductances of colonic crypts from dexamethasone-treated rats. Pflügers Arch 431:419–426

Fischer H, Illek B, Finkbeiner WE, Widdicombe JH (2007) Basolateral Cl channels in primary airway epithelial cultures. Am J Physiol Lung Cell Mol Physiol 292:L1432–L1443

Geibel JP (2005) Secretion and absorption by colonic crypts. Annu Rev Physiol 67:471–490

Gründer S, Thiemann A, Pusch M, Jentsch TJ (1992) Regions involved in the opening of CIC-2 chloride channel by voltage and cell volume. Nature 360:759–762

Gu Y (2008) Effect of $[Cl^-]_i$ on ENaC activity from mouse cortical collecting duct cells. J Cell Physiol 216:453–457

Gyömörey K, Yeger H, Ackerley C, Garami E, Bear CE (2000) Expression of the chloride channel ClC-2 in the murine small intestine epithelium. Am J Physiol Cell Physiol 279:C1787–C1794

Hinzpeter A, Lipecka J, Brouillard F, Baudoin-Legros M, Dadlez M, Edelman A, Fritsch J (2006) Association between Hsp90 and the ClC-2 chloride channel upregulates channel function. Am J Physiol Cell Physiol 290:C45–C56

Hinzpeter A, Fritsch J, Borot F, Trudel S, Vieu DL, Brouillard F, Baudouin-Legros M, Clain J, Edelman A, Ollero M (2007) Membrane cholesterol content modulates ClC-2 gating and sensitivity to oxidative stress. J Biol Chem 282:2423–2432

Inagaki A, Yamaguchi S, Ishikawa T (2004a) Amiloride-sensitive epithelial Na^+ channel currents in surface cells of rat rectal colon. Am J Physiol Cell Physiol 286:C380–C390

Inagaki A, Yamaguchi S, Ishikawa T (2004b) Functional expression of ENaC and ClC-2-like channel in surface cells of rat rectal colon. Jpn J Physiol 54(Suppl):S58

Jacobi C, Leipziger J, Nitschke R, Ricken S, Greger R (1998) No evidence for cell-to-cell coupling in rat colonic crypts: studies with Lucifer Yellow and with photobleaching. Pflügers Arch 436:83–89

Jentsch TJ, Stein V, Weinreich F, Zdebik AA (2002) Molecular structure and physiological function of chloride channels. Physiol Rev 82:503–568

Kunzelmann K (2003) ENaC is inhibited by an increase in the intracellular Cl^- concentration mediated through activation of Cl^- channels. Pflügers Arch 445:504–512

Kunzelmann K, Mall M (2002) Electrolyte transport in the mammalian colon: mechanisms and implications for disease. Physiol Rev 82:245–289

Lipecka J, Bali M, Thomas A, Fanen P, Edelman A, Fritsch J (2002) Distribution of ClC-2 chloride channel in rat and human epithelial tissues. Am J Physiol Cell Physiol 282:C805–C816

Lomax RB, McNicholas CM, Lombes M, Sandle GI (1994) Aldosterone-induced apical Na^+ and K^+ conductances are located predominantly in surface cells in rat distal colon. Am J Physiol 266:G71–G82

Moeser AJ, Haskell MM, Shifflett DE, Little D, Schultz BD, Blikslager AT (2004) ClC-2 chloride secretion mediates prostaglandin-induced recovery of barrier function in ischemia-injured porcine ileum. Gastroenterology 127:802–815

Nehrke K, Arreola J, Nguyen HV, Pilato J, Richardson L, Okunade G, Baggs R, Shull GE, Melvin JE (2002) Loss of hyperpolarization-activated Cl^- current in salivary acinar cells from Clcn2 knockout mice. J Biol Chem 277:23604–23611

Niemeyer MI, Yusef YR, Cornejo I, Flores CA, Sepúlveda FV, Cid LP (2004) Functional evaluation of human ClC-2 chloride channel mutations associated with idiopathic generalized epilepsies. Physiol Genomics 19:74–83

Niemeyer MI, Cid LP, Yusef YR, Briones R, Sepúlveda FV (2009) Voltage-dependent and -independent titration of specific residues accounts for complex gating of a ClC chloride channel by extracellular protons. J Physiol 587:1387–1400

Nobile M, Pusch M, Rapisarda C, Ferroni S (2000) Single-channel analysis of a ClC-2-like chloride conductance in cultured rat cortical astrocytes. FEBS Lett 479:10–14

Park K, Arreola J, Begenisich T, Melvin JE (1998) Comparison of voltage-activated Cl^- channels in rat parotid acinar cells with ClC-2 in a mammalian expression system. J Membr Biol 163: 87–95

Peña-Münzenmayer G, Catalán M, Cornejo I, Figueroa CD, Melvin JE, Niemeyer MI, Cid LP, Sepúlveda FV (2005) Basolateral localization of native ClC-2 chloride channels in absorptive intestinal epithelial cells and basolateral sorting encoded by a CBS-2 domain di-leucine motif. J Cell Sci 118:4243–4252

Pusch M, Jordt SE, Stein V, Jentsch TJ (1999) Chloride dependence of hyperpolarization-activated chloride channel gates. J Physiol 515:341–353

Romanenko VG, Nakamoto T, Catalán MA, Gonzalez-Begne M, Schwartz GJ, Jaramillo Y, Sepúlveda FV, Figueroa CD, Melvin JE (2008) Clcn2 encodes the hyperpolarization-activated chloride channel in the ducts of mouse salivary glands. Am J Physiol Gastrointest Liver Physiol 295:G1058–G1067

Thiemann A, Gründer S, Pusch M, Jentsch TJ (1992) A chloride channel widely expressed in epithelial and non-epithelial cells. Nature 356:57–60

Varela D, Niemeyer MI, Cid LP, Sepúlveda FV (2002) Effect of an N-terminus deletion on voltage-dependent gating of the ClC-2 chloride channel. J Physiol 544:363–372

Weinreich F, Jentsch TJ (2001) Pores formed by single subunits in mixed dimers of different CLC chloride channels. J Biol Chem 276:2347–2353

Xie Y, Schafer JA (2004) Inhibition of ENaC by intracellular Cl^- in an MDCK clone with high ENaC expression. Am J Physiol Renal Physiol 287:F722–F731

Xiong H, Li C, Garami E, Wang Y, Ramjeesingh M, Galley K, Bear CE (1999) ClC-2 activation modulates regulatory volume decrease. J Membr Biol 167:215–221

Zdebik AA, Cuffe JE, Bertog M, Korbmacher C, Jentsch TJ (2004) Additional disruption of the ClC-2 Cl^- channel does not exacerbate the cystic fibrosis phenotype of cystic fibrosis transmembrane conductance regulator mouse models. J Biol Chem 279:22276–22283